An Extension of the Kinetic Battery Model for Optimal Control Applications

1st Masoomeh Karami
Department of Computing
University of Turku
Turku, Finland
Valmet Automotive EV Power
Turku, Finland
mkaram@utu.fi

2nd Sajad Shahsavari
Department of Computing
University of Turku
Turku, Finland
Computational Eng. and Analysis
Turku University of Applied Sciences
Turku, Finland
sajsha@utu.fi

3rd Eero Immonen
Computational Eng. and Analysis
Turku University of Applied Sciences
Turku, Finland
eero.immonen@turkuamk.fi

4th Mohammad-Hashem Haghbayan
Department of Computing
University of Turku
Turku, Finland
mohhag@utu.fi

5th Juha Plosila
Department of Computing
University of Turku
Turku, Finland
juplos@utu.fi

***Abstract*—Optimal control of electric vehicle (EV) batteries for maximal energy efficiency, safety and lifespan requires that the Battery Management System (BMS) has accurate real-time information on both the battery State-of-Charge (SoC) *and its dynamics*, i.e. energy supply capacity, at all times. However, these quantities cannot be measured directly from the battery, and, in practice, only SoC estimation is typically carried out. Moreover, the so-called Equivalent Circuit Models (ECM) commonly utilized in BMS solutions only display a memoryless algebraic dependence of voltage and current on SoC, without an ability to predict battery energy supply capacity based on its recent charge/discharge history. In this article, we propose a novel parametric algebraic voltage model coupled to the well-known Manwell-McGowan dynamic Kinetic Battery Model (KiBaM), which is able to predict both battery SoC dynamics and its electrical response. We present an offline model parameter identification procedure that yields SoC-dependent model parameters from standard dynamic battery tests, and we introduce an algorithm based on the Extended Kalman Filter (EKF) for standard SoC estimation on the proposed model. Numerical simulations, based on laboratory measurements, are presented for prismatic Lithium-Titanate Oxide (LTO) battery cells. Such cells are prime candidates for modern heavy offroad EV applications.**

***Index Terms*—Energy Storage Systems, Battery Management, KiBaM model, Battery state-of-charge.**

I. Introduction

Lithium-ion batteries, typically composed of several interconnected cells, are important for modern energy storage and mobility applications, because they can help to combat the climate change. For example, the net lifetime emissions of hybrid and electric vehicles have been reported to be up to 89% lower than for internal combustion engine vehicles [1]. In practice, though, batteries can be inefficient and be made of raw materials that have high environmental and energy impacts [2]. Recently, researchers have increasingly been focusing on *optimal control* problems for battery powered *smart systems* to increase their energy efficiency, safety and lifetime — and thus reduce their environmental impact (e.g., [3]–[5]). Such smart systems are typically equipped with an implicit *digital twin* of the energy source, i.e., models that mathematically represent the physical dynamics and constraints in different cycling situations, which are the focus of this article.

A substantial challenge in optimal control of battery systems is that the energy content is not directly measurable outside the battery. Indeed, in practice, mathematical modeling of battery energy dynamics in different charge and discharge conditions has to be based on electrical, i.e. voltage (V) and current (I), measurements. Typically, these measurements are utilized to first identify an Equivalent Circuit Model (ECM) that predicts the electrical response of the battery (see e.g. [6]–[9] and the references therein). For run-time state estimation, the ECM model is then typically coupled to a simple SoC model, such as Coulomb counting or its derivatives [10]. This approach has been demonstrated to yield remarkably accurate estimates of the SoC during battery operation by many researchers (see e.g. [11]–[13]). However, it is important to emphasize that the SoC estimate thus obtained is *static* and *memoryless*: It does not address the effect of the recent past usage history of the battery on the energy (or power) available from that battery in the immediate future. This missing information, namely dynamic performance bounds on the battery based on the available capacity, is crucial for energy-optimal control of the battery, and is addressed in the present work.

In this article, we take an opposite battery modeling approach relative to that described above: We propose a simple algebraic electrical subsystem model coupled to a more

complex dynamical model of the energy subsystem. The energy model considered herein is the Kinetic Battery Model (KiBaM) specification introduced by Manwell and McGowan in 1993 [14], see Fig. 1(a). It is well known to be able to represent the recovery and rate-capacity effects seen in real batteries [15], among others. The challenge with the KiBaM model is relating it to the battery voltage and current, which is necessary for parameter identification and practical use. Manwell et al. [16] proposed the simple algebraic specification $V = V_{oc} - R_s I$, where V_{oc} denotes the open-circuit voltage and R_s the internal resistance of the battery, but without relation to SoC. Further, Bako et al. [17] and Manwell et al. [16] proposed a rational voltage models with SoC dependence. On the other hand, Fenner et al. [18] proposed a parametric rational-exponential voltage law targeted at replicating the response seen in constant current discharge tests. However, the nonlinearities in these electrical subsystem models potentially make parameter identification complex, and also impose a heavier computational burden on the battery SoC estimation during runtime. It is, therefore, of considerable theoretical and practical interest to establish a simple and computationally lightweight but accurate electrical subsystem model to be augmented with the KiBaM model. Such a model is presented herein, along with its offline parameter identification method, which utilizes standard dynamic discharge profile laboratory test data [19]. Moreover, we present an algorithm, based on the extended Kalman filter (EKF) to estimate the unknown internal states of the battery based on real-world measurements. As an application, we consider LTO battery cells that are the prime candidates for heavy off-road electric vehicles due to their robustness to high currents, repeated cycling and operation in cold temperatures [19], [20]. The presented numerical results for LTO cells show that the out-of-sample voltage prediction for the proposed model is in good agreement with the measurement data, and EKF-based SoC estimation converges to the true SoC accurately and quickly. As a consequence, the presented model and estimation method are potentially useful as such in modern electric vehicle Battery Management Systems (BMS). More importantly, presented method is also capable of estimating the internal *dynamics* of the battery energy system, providing necessary information for optimal control applications in mobile resource-constrained smart systems.

This paper is based on the preliminary idea in [21] that is an extended abstract. In the current paper, we enhance the work by utilizing extended Kalman filter to estimate the internal hidden states of the model based on measurable input and output of the battery system. This gives us capability to estimate the battery parameters while the initial state of the battery is unknown. Moreover, we elaborate the description and formulations of the battery models along with comprehensive discussion on the obtained results.

II. Battery Model

We employ Kinetic Battery Model (KiBaM) to model the electro-chemical dynamics of battery's internal states and represent the energy/charge balance. Then, we introduce a simple linear voltage model to predict battery's terminal voltage based on its energy/charge state.

A. Kinetic Battery Model

Fig. 1(a) illustrates the structure of the well-known KiBaM that resembles the charge in the battery to liquid split into two tanks, i.e., the *bound charge* tank and the *available charge* tank, attached through a limited-rate valve. The liquid volume represents the battery charge and the flow represents current. Variables y_1 and y_2 show the amount of *available charge* and *bound charge*, respectively. The relative capacity of the tanks is specified by the parameter $c \in (0, 1)$. Additionally, parameter k controls the flow rate: amount of charge transferred from bound to available charge tank (or vice versa) based on their height difference. The dynamics of charge in each tank is modeled by the following differential equations:

$$\frac{dy_1}{dt} = \frac{k}{1-c} y_2(t) - \frac{k}{c} y_1(t) - I(t) \tag{1a}$$

$$\frac{dy_2}{dt} = -\frac{k}{1-c} y_2(t) + \frac{k}{c} y_1(t) \tag{1b}$$

We defined the battery SoC level at each time by:

$$SoC(t) = \frac{y_1(t) + y_2(t)}{Q_0} \tag{2}$$

where Q_0 is the nominal capacity of the battery.

In this model, variables y_1 and y_2 are the measures of energy level in the battery, while in practice, these values cannot be measured and measurements are restricted only to the battery instantaneous terminal voltage and applied current. Therefore, an energy-to-voltage conversion model is needed to relate the energy measures to voltage predictions.

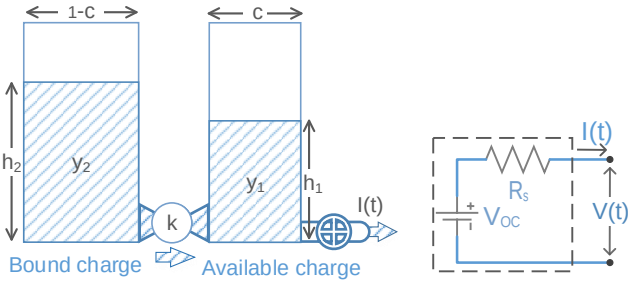

(a) KiBaM (b) Rint model

Fig. 1. Conceptual illustration of the KiBaM and circuit model

B. Voltage Model

Our proposed voltage model is a linearly parameterized equation describing voltage response of the battery based on the Rint equivalent circuit model [22] (Fig. 1(b)). Having the values of KiBaM states (available and bound SoC, Eq. 2), terminal voltage $V(t)$ at time t is modeled by the equation:

$$V(t) = V_{OC} - R_s \cdot I(t) + E_0 + E_1 \cdot \frac{y_1(t)}{Q_0} + E_2 \cdot \frac{y_2(t)}{Q_0} \tag{3}$$

where R_s is the battery internal resistance, V_{OC} is the battery open-circuit voltage and E_0, E_1 and E_2 are the parameters of the linear voltage model.

It is essential to mention that, in our experiments, parameters of Rint, KiBaM and voltage model are all dependent on current SoC level. Therefore, all should be subscripted with $SoC(t)$ in equations 1a, 1b and 3, but for notational convenience, this dependence is not explicitly denoted.

III. Parameter Identification

To use the model in equations (1)-(3) in practice, we must identify the parameters c, k, E_0, E_1 and E_2 so that the predicted voltage in Eq. (3) and predicted SoC in Eq. (2) are close to those seen in laboratory measurements. It has been experimentally verified for many different battery chemistries that V_{OC} and R_s are SoC-dependent. Consequently, it makes sense to also allow for SoC-dependence in c, k, E_0, E_1 and E_2.

The training data $\mathcal{D}_{train}$ for parameter identification consists of measurement data as follows:

$$\mathcal{D}_{train} = \{(I_i(t), V_i(t), SoC_i(t)) \mid t \in [0, T_i], i = 1 \cdots N\} \tag{4}$$

as a set of triplets: measured current, voltage and SoC profiles, for different N experiments. The battery is assumed to be fully charged at the beginning of each experiment, current profile $I_i(t)$ is applied and battery's terminal voltage $V_i(t)$ and capacity change are observed at discrete times. Note that the capacity change is measured in terms of ampere hours and $SoC_i(t)$ is calculated based on its integration divided by nominal capacity.

For model identification, we aim to minimize the multivariate constrained error function $e(p)$ defined as:

$$e(p) = \sum_{i=0}^{N} \|V_i(t) - \hat{V}_i^p(t)\| \tag{5}$$

w.r.t. the model parameters $p = (c, k, E_0, E_1, E_2)$, subject to inequality conditions $0 \leq y_1 \leq cQ_0$ and $0 \leq y_2 \leq (1-c)Q_0$, where $V_i(t)$ is measured voltage and $\hat{V}_i^p(t)$ is the predicted voltage via parameter set p at time t. The optimization is performed only using measured voltage data, but the model implicitly provides an accurate fit on SoC data, due to the imposed model constraints.

The objective (5) can be minimized by using the interior-point optimization method [23]. However, to mitigate the effect of choice of initial point in parametric interior point optimization, we propose a four-stage procedure, described below. It consists of first establishing a reasonable initial point incrementally and then seeking an optimal parameter set starting from that point. The first three stages seek parameters that do not depend on SoC, whereas the last stage addresses SoC dependence. The stages of parameter identification procedure are as follows:

1) First, Eq. 2 is used to predict the SoC level and *only* the KiBaM parameters c and k are identified by fitting predicted SoC to the measured SoC on the whole training dataset (by minimizing the SoC error function similar to voltage as described in Eq. 5).
2) Then, Eq. 3 is exploited to predict the terminal voltage with fixed KiBaM parameters c and k (the solution of stage 1) and then *only* the voltage model parameters E_0, E_1 and E_2 are identified by fitting the predicted voltage and measured voltage on the whole training dataset.
3) Afterwards, the solution of the previous two stages are used as the starting point and the interior-point optimization is run for identifying *all* parameters c, k, E_0, E_1 and E_2 by fitting the predicted voltage and measured voltage on the whole training dataset, exactly as represented in Eq. (5).
4) Finally, for the SoC-dependent parameters, the SoC range (0-to-100%) is divided into K equal subranges, and for each subrange the corresponding voltage and current data are extracted. Then, the optimization procedure is performed for each subrange (starting from the SoC-independent parameters found in stage 3). Subsequently, the optimal parameter set of each subrange is assigned to its centeral SoC value. These K optimal parameter samples are used to linearly interpolate the whole SoC range (see figure 3 for the demonstration).

The validation phase is mainly computing the error function in Eq. (5) for the optimal parameter set over validation dataset $\mathcal{D}_{val}$. The validation dataset is similar to training dataset in shape. However, since the model should perform well on any applied current, the current (and consequently, measured terminal voltage and SoC) profiles are different in the validation dataset (out-of-sample data).

IV. State-of-charge Estimation

In this paper, we also propose a model-based state estimation method, as a practical application of our developed battery model, by using extended Kalman filters (EKF) [24]. Algorithm 1 describes the EKF-based SoC estimation. The objective is to estimate the unknown internal state of the KiBaM dynamical system, i.e., available and bound charges $(y_1(t), y_2(t))$, only by observing measurable signals $I(t)$ and $V(t)$. The inputs are optimized SoC-dependent parameter set (Section III) and measured current and voltage profiles. Starting from an initial state value (Line 1), the update rule of EKF (Lines 8-16) tries to minimize the error between estimated voltage V_{pred} and measured voltage $\mathbf{V}[t]$ (Line 12) at each time step. We used the Jacobian of dynamical model (KiBaM) and Jacobian of measurement model (voltage), F and H respectively, as:

$$F = I_2 + dt \cdot \begin{bmatrix} -k/c & k/(1-c) \\ k/c & -k/(1-c) \end{bmatrix} \tag{6}$$

$$H = \frac{(\Delta V_{OC} - \Delta R_s) \cdot I(t)}{Q_0} \cdot \begin{bmatrix} E_1 & E_2 \end{bmatrix} \tag{7}$$

where ΔV_{OC} and ΔR_s are derivatives of V_{OC} and R_s w.r.t. state (y_1, y_2), which are computed programmatically. Finally,

Algoritm 1 Extended Kalman filter for SoC estimation

Input: $\mathbf{params}$, $\mathbf{I}$, $\mathbf{V}$
Output: SoC

$\mathbf{y} \leftarrow [y_1^{init}, y_2^{init}]$
$t \leftarrow 0$
$\mathbf{P} \leftarrow I_2$ ▷ Identity Matrix
$Q, R, dt \leftarrow$ constant
while TRUE **do**
  $SoC[t] \leftarrow sum(\mathbf{y})/Q_0$
  $\mathbf{param_{soc}} \leftarrow \mathbf{params}[SoC[t]]$
  $\mathbf{F}, \mathbf{H} \leftarrow$ MODELJACOBIANS($\mathbf{param_{soc}}, \mathbf{I}[t], dt$) ▷ Eq. 6, 7
  $\mathbf{y}^- \leftarrow$ KIBAMSTEP($\mathbf{param_{soc}}, \mathbf{y}, \mathbf{I}[t], dt$) ▷ Eq. 1a, 1b
  $\mathbf{P}^- \leftarrow \mathbf{FPF}^\mathsf{T} + Q$
  $V_{pred} \leftarrow$ VOLTAGEMODEL($\mathbf{param_{soc}}, \mathbf{y}^-, \mathbf{I}[t]$) ▷ Eq. 3
  $v \leftarrow \mathbf{V}[t] - V_{pred}$
  $\mathbf{S} \leftarrow \mathbf{HP}^-\mathbf{H}^\mathsf{T} + R$
  $\mathbf{K} \leftarrow \mathbf{P}^-\mathbf{H}^\mathsf{T}\mathbf{S}^{-1}$
  $\mathbf{y} \leftarrow \mathbf{y}^- + \mathbf{K}v$
  $\mathbf{P} \leftarrow \mathbf{P}^- - \mathbf{KSK}^\mathsf{T}$
  $t \leftarrow t + dt$
end while

TABLE I
SPECIFICATIONS OF THE BATTERY CELL

Type	Prismatic high-energy cell	**Anode material**	LTO
Rated capacity	23Ah	**Nominal Voltage**	2.3V
Lower cutoff voltage	1.5V	**Upper cutoff voltage**	2.7V

process noise (Q) and measurement noise (R) are assumed to be Gaussian random noise with constant amplitude.

V. EXPERIMENTS

In this section, we explain details of the conducted experiments, e.g., specifications of battery cell of interest, datasets, results of parameter identification and model validations, and finally the results for battery SoC estimation.

A. Battery specifications and dataset

The battery cell considered herein is a prismatic high-energy 23Ah Toshiba SCiB^{TM} LTO battery cell, with 1.5V and 2.7V as lower and upper cutoff voltage, respectively (Table I). To train the model and validate the results, we used data from Discharge Pulse Power Characterization (DPPC) tests [19] which are common tests to capture the battery cell's dynamics in response to repeatedly changing discharge current. The test was performed in room temperature at two different charge rates (which will be referred to by "1C" and "4C" C-rates). The C-rate refers to the speed charging/discharging relative to battery's rated capacity. 1C means that the battery is charged/discharged from 0% to 100% in 1 hour. We refer the reader to [19], [25] for detailed description of battery specification and DPPC tests. We used 1C data as the training dataset for parameter identification and 4C dataset for model validation (shown by red in Figures 2(a) and 2(b), respectively).

B. Parameter identification and validation

For identifying five parameters of the KiBaM and voltage model (Section III), we implemented the KiBaM differential equations and voltage model and imposed model constraints in MATLAB code, and then used MATLAB built-in nonlinear optimization method `fmincon` to find minimum of the constrained nonlinear multivariable error function in Eq. 5. The optimization is performed over 1C training data and the 0-to-100% range of SoC is divided into $K = 10$ equal subranges. The Rint model parameters V_{OC} and R_s are determined based on the voltage drop caused by applied non-zero current immediately after a rest period in DPPC test. By definition, this drop occurs because of the algebraic part of Eq. (3) which depends on the internal resistance, therefore according to the *Ohm's law*, $R_s = (V_a - V_b)/I$ (V_a being the voltage at top, and V_b the voltage at the bottom of the drop). The optimized parameters are presented in Fig. 3 as functions of SoC. The change in SoC-dependent parameters show that the battery behaves significantly differently at various SoC levels. Considering the parameter k, for example, Fig. 3 shows that, interestingly, when the battery is full, the charge transfer rate from the bound charge tank to available charge tank is higher than when it is drained, thus faster energy recovery can obtained at fully charge. Additionally, the trend in parameter c suggests that the bound charge tank is used to store the charge as a reserved energy unit which is released as the SoC drops. Trends in V_{OC} and R_s are as expected, and E_0 almost similar trend to V_{OC}, affecting the predicted voltage as a correction value for V_{OC}. Also, the negative range in E_2 supports the fact that in order to utilize the charge in the bound tank, it must be first transferred to available tank. This is evident in the voltage increase in the recovery effect, when the battery is let to rest after a non-zero current, and transferring charge from bound to available tank increases the voltage response.

Fig. 2 shows the SoC and voltage predictions of the optimized model over 1C and 4C data. It can be observed that the model is able to predict the SoC and voltage of the battery with high accuracy for in-sample and out-of-sample data. Table V-B contains the mean and max percentage and absolute errors for optimized voltage response model. We compared MPE of the proposed method to the published results in [19], with relative improvement of 54% and 80% on voltage prediction accuracy over training and validation datasets, respectively.

TABLE II
VOLTAGE PREDICTION PERFORMANCE, IN TERMS OF MAX AND MEAN PERCENTAGE AND ABSOLUTE ERROR.

	Max % Error	Mean % Error	Max Abs. Error (V)	Mean Abs. Error (V)
Training	0.88%	0.092%	0.0228	0.0021
Validation	1.20%	0.065%	0.0297	0.0016

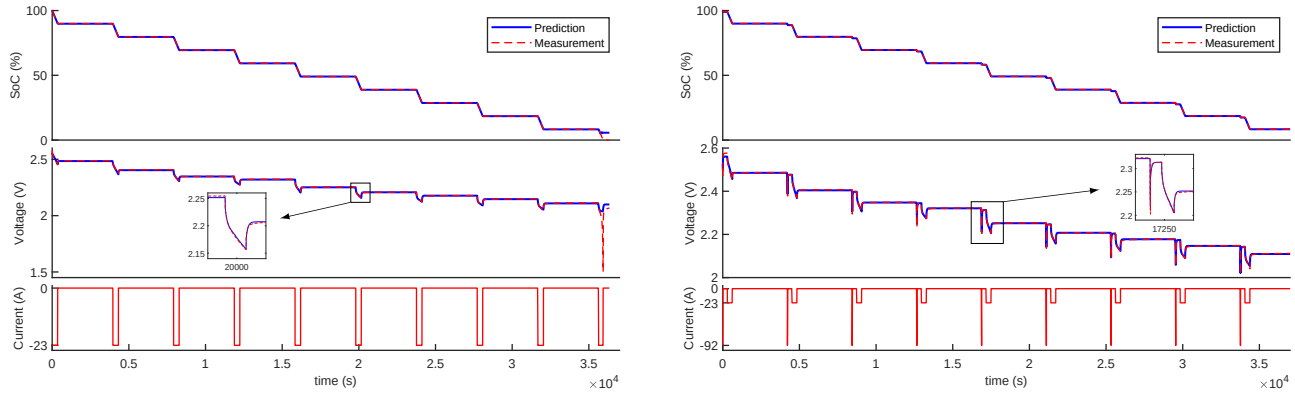

(a) In-sample 1C data

(b) Out-of-sample 4C data

Fig. 2. Performance of SoC and voltage prediction over in-sample (1C, in the left) and out-of-sample (4C, right) data, computed using optimized parameter set..

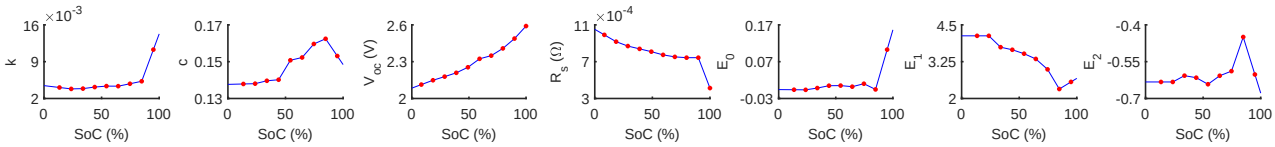

Fig. 3. KiBaM parameters (k, c) and voltage model parameters (E_0, E_1, E_2, V_{oc}, R_s) over SoC level. Red points indicate the optimized parameters of each subrange and blue lines indicate their linear interpolation over the whole range of SoC [21].

C. Application: EKF for SoC estimation

The results of the SoC estimation using EKF is presented in Fig. 4 for 1C and 4C datasets with different initial values for unknown model state. The plots show that the proposed EKF-based state estimation method is able to converge to the actual SoC value after a transient period (shown as close-up view inside the plots in Fig. 4), regardless of the initial value. The high variation in the estimated value in this period is due to the model SoC-dependent parameters, which are varying as the estimated SoC is changing. Nevertheless, after convergence, the estimated state steadily follows the actual state dynamics. Table V-C shows the mean percentage and absolute errors and the convergence time of SoC estimation with 60% initial state and 1 Hz sampling frequency. We define the convergence time as the first time that the error between estimated SoC and true SoC is within the 5% error bound (similar to [26]). The transition period can be shortened by better initialization of SoC value or increasing sampling frequency to achieve faster convergence.

TABLE III
EKF PERFORMANCE, IN TERMS OF MEAN PERCENTAGE AND ABSOLUTE ERROR AND CONVERGENCE TIME OF SOC ESTIMATION, INITIALIZED FROM SOC 60% AND ON 1HZ SAMPLING FREQUENCY.

	Mean % Error	**Mean Abs. Error**	**Convergence time (Sec)**
1C SoC	0.76%	0.28%	46
4C SoC	0.23%	0.12%	43

VI. CONCLUSION

In this article, we introduced a novel light-weight voltage model based on the battery internal energy dynamics represented by KiBaM. Also, a four-stage parameter identification procedure based on interior-point constrained optimization is described that avoids local convergence and provides high voltage prediction accuracy on out-of-sample data due to our SoC-dependent parameter scheme. We successfully applied our optimized model on the fundamental SoC estimation problem by using extended Kalman filter. The estimated output of the proposed algorithm is converged to the true SoC value shortly and accurately. In the proposed model, the effect of operation temperature on the battery's voltage response is not considered. Also, battery aging is not considered in this work which is another factor that affects model parameters. However, designing such temperature- and aging-dependant parameters (given the training dataset) is technically feasible with the proposed parameter identification procedure. One interesting future direction of this work is to utilize this battery model and SoC-estimation in optimal control of resource-constrained mobile robots. Specifically,

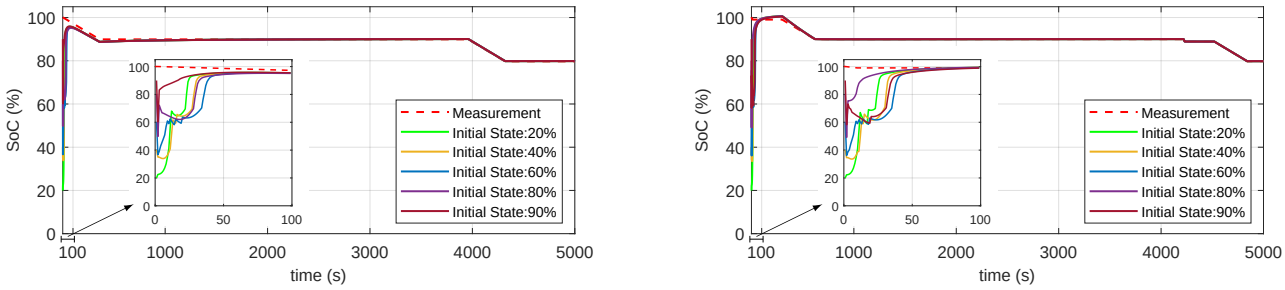

(a) 1C data

(b) 4C data

Fig. 4. Estimation of SoC using extended Kalman filtering with different (guessed) initial states.

proposed battery model can be integrated into robotic control systems to address energy-efficient resource-aware operation planning. Additionally, studying parameter drift and effect of temperature and aging on the battery model is another future direction.

REFERENCES

[1] J. Buberger, A. Kersten, M. Kuder, R. Eckerle, T. Weyh, and T. Thiringer, "Total co2-equivalent life-cycle emissions from commercially available passenger cars," *Renewable and Sustainable Energy Reviews*, vol. 159, p. 112158, 2022.

[2] M. C. McManus, "Environmental consequences of the use of batteries in low carbon systems: The impact of battery production," *Applied Energy*, vol. 93, pp. 288–295, 2012.

[3] H. Dong, H. Zhang, F. Ding, H. Tan, and J. Peng, "Battery-aware cooperative merging strategy of connected electric vehicles based on reinforcement learning with hindsight experience replay," *IEEE Transactions on Transportation Electrification*, 2021.

[4] D. M. Rosewater, D. A. Copp, T. A. Nguyen, R. H. Byrne, and S. Santoso, "Battery energy storage models for optimal control," *IEEE Access*, vol. 7, pp. 178 357–178 391, 2019.

[5] D. Baek, Y. Chen, A. Bocca, L. Bottaccioli, S. Di Cataldo, V. Gatteschi, D. J. Pagliari, E. Patti, G. Urgese, N. Chang *et al.*, "Battery-aware operation range estimation for terrestrial and aerial electric vehicles," *IEEE Transactions on Vehicular Technology*, vol. 68, no. 6, pp. 5471–5482, 2019.

[6] X. Zhang, W. Zhang, and G. Lei, "A review of li-ion battery equivalent circuit models," *Transactions on Electrical and Electronic Materials*, vol. 17, no. 6, pp. 311–316, 2016.

[7] S. Nejad, D. Gladwin, and D. Stone, "A systematic review of lumped-parameter equivalent circuit models for real-time estimation of lithium-ion battery states," *Journal of Power Sources*, vol. 316, pp. 183–196, 2016.

[8] S. Tamilselvi, S. Gunasundari, N. Karuppiah, A. Razak RK, S. Madhusudan, V. M. Nagarajan, T. Sathish, M. Z. M. Shamim, C. A. Saleel, and A. Afzal, "A review on battery modelling techniques," *Sustainability*, vol. 13, no. 18, p. 10042, 2021.

[9] M. Tomasov, M. Kajanova, P. Bracinik, and D. Motyka, "Overview of battery models for sustainable power and transport applications," *Transportation Research Procedia*, vol. 40, pp. 548–555, 2019.

[10] K. S. Ng, C.-S. Moo, Y.-P. Chen, and Y.-C. Hsieh, "Enhanced coulomb counting method for estimating state-of-charge and state-of-health of lithium-ion batteries," *Applied energy*, vol. 86, no. 9, pp. 1506–1511, 2009.

[11] C. Zhang, K. Li, S. Mcloone, and Z. Yang, "Battery modelling methods for electric vehicles-a review," in *2014 European Control Conference (ECC)*. IEEE, 2014, pp. 2673–2678.

[12] D. N. How, M. Hannan, M. H. Lipu, and P. J. Ker, "State of charge estimation for lithium-ion batteries using model-based and data-driven methods: A review," *Ieee Access*, vol. 7, pp. 136 116–136 136, 2019.

[13] W. Zhou, Y. Zheng, Z. Pan, and Q. Lu, "Review on the battery model and soc estimation method," *Processes*, vol. 9, no. 9, p. 1685, 2021.

[14] J. F. Manwell and J. G. McGowan, "Lead acid battery storage model for hybrid energy systems," *Solar Energy*, vol. 50, no. 5, pp. 399–405, 1993.

[15] Z. N. Bako, M. A. Tankari, G. Lefebvre, and A. S. Maiga, "Experiment-based methodology of kinetic battery modeling for energy storage," *IEEE Transactions on Industry Applications*, vol. 55, no. 1, pp. 593–599, 2018.

[16] J. F. Manwell, J. G. McGowan, U. Abdulwahid, and K. Wu, "Improvements to the hybrid2 battery model," in *Windpower 2005 Conference*, 2005.

[17] Z. N. Bako, M. A. Tankari, G. Lefebvre, and A. S. Maiga, "Lead-acid battery behavior study and modelling based on the kinetic battery model approach," in *2016 IEEE International Conference on Renewable Energy Research and Applications (ICRERA)*. IEEE, 2016, pp. 673–677.

[18] G. P. Fenner, L. F. Ramos, and L. N. Canha, "Battery analysis using kinetic battery model with voltage response," in *2020 55th International Universities Power Engineering Conference (UPEC)*. IEEE, 2020, pp. 1–5.

[19] E. Immonen and J. Hurri, "Equivalent circuit modeling of a high-energy lto battery cell for an electric rallycross car," in *2021 IEEE 30th International Symposium on Industrial Electronics (ISIE)*, 2021, pp. 1–5.

[20] J. Mei, E. K. W. Cheng, and Y. C. Fong, "Lithium-titanate battery (lto): A better choice for high current equipment," in *2016 International Symposium on Electrical Engineering (ISEE)*, 2016, pp. 1–4.

[21] M. Karami, S. Shahsavari, E. Immonen, H. Haghbayan, and J. Plosila, "A Coupled Battery State-of-Charge and Voltage Model for Optimal Control Applications," in *Proc. Conf. Design, Automation & Test in Europe (DATE)*, 2023.

[22] P. Shen, M. Ouyang, L. Lu, J. Li, and X. Feng, "The co-estimation of state of charge, state of health, and state of function for lithium-ion batteries in electric vehicles," *IEEE Transactions on Vehicular Technology*, vol. 67, no. 1, pp. 92–103, 2018.

[23] J. Nocedal, F. Öztoprak, and R. A. Waltz, "An interior point method for nonlinear programming with infeasibility detection capabilities," *Optimization Methods and Software*, vol. 29, no. 4, pp. 837–854, 2014.

[24] Y. Bar-Shalom, X. R. Li, and T. Kirubarajan, *Estimation with applications to tracking and navigation: theory algorithms and software*. John Wiley & Sons, 2004.

[25] E. Immonen and J. Hurri, "Incremental thermo-electric cfd modeling of a high-energy lithium-titanate oxide battery cell in different temperatures: A comparative study," *Applied Thermal Engineering*, vol. 197, p. 117260, 2021.

[26] Z. Wei, C. Zou, F. Leng, B. H. Soong, and K.-J. Tseng, "Online model identification and state-of-charge estimate for lithium-ion battery with a recursive total least squares-based observer," *IEEE Transactions on Industrial Electronics*, vol. 65, no. 2, pp. 1336–1346, 2017.